

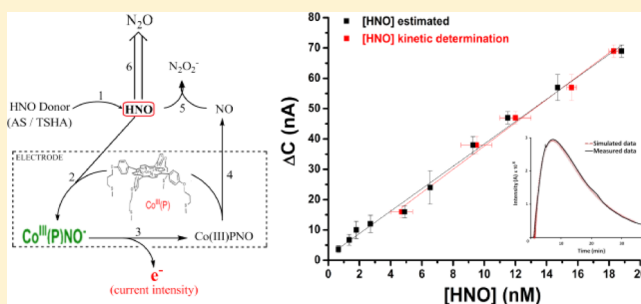
# Time-Resolved Electrochemical Quantification of Azanone (HNO) at Low Nanomolar Level

Sebastián A. Suárez,<sup>†</sup> Damian E. Bikiel,<sup>†</sup> Diana E. Wetzler,<sup>‡</sup> Marcelo A. Martí,<sup>\*,†,‡</sup> and Fabio Doctorovich<sup>\*,†</sup>

<sup>†</sup>Departamento de Química Inorgánica, Analítica y Química Física/INQUIMAE-CONICET, and <sup>‡</sup>Departamento de Química Biológica, Facultad de Ciencias Exactas y Naturales, Universidad de Buenos Aires, Ciudad Universitaria, Pab. II, C1428EHA, Buenos Aires, Argentina

## Supporting Information

**ABSTRACT:** Azanone (HNO, nitroxyl) is a highly reactive and short-lived compound with intriguing and highly relevant properties. It has been proposed to be a reaction intermediate in several chemical reactions and an in vivo, endogenously produced key metabolite and/or signaling molecule. In addition, its donors have important pharmacological properties. Therefore, given its relevance and elusive nature (it reacts with itself very quickly), the development of reliable analytical methods for quantitative HNO detection is in high demand for the advancement of future research in this area. During the past few years, several methods were developed that rely on chemical reactions followed by mass spectrometry, high-performance liquid chromatography, UV–vis, or fluorescence-trapping-based methodologies. In this work, our recently developed HNO-sensing electrode, based on the covalent attachment of cobalt(II) 5,10,15,20-tetrakis[3-(*p*-acetylthiopropoxy)phenyl] porphyrin [Co(P)] to a gold electrode, has been thoroughly characterized in terms of sensibility, accuracy, time-resolved detection, and compatibility with complex biologically compatible media. Our results show that the Co(P) electrode: (i) allows time-resolved detection and kinetic analysis of the electrode response (the underlying HNO-producing reactions can be characterized) (ii) is able to selectively detect and reliably quantify HNO in the 1–1000 nM range, and (iii) has good biological media compatibility (including cell culture), displaying a lack of spurious signals due to the presence of O<sub>2</sub>, NO, and other reactive nitrogen and oxygen species. In summary, the Co(P) electrode is to our knowledge the best prospect for use in studies investigating HNO-related chemical and biological reactions.



Azanone (HNO), also called nitroxyl, is a highly reactive and short-lived compound with intriguing and highly relevant chemical and biological properties.<sup>1,2</sup> HNO biological targets are mainly thiols<sup>2,3</sup> and metalloproteins, especially heme proteins.<sup>4–7</sup> HNO also reacts with oxygen, NO, and itself in a reaction that is extremely fast, and therefore, the maximum concentration and lifetime of azanone are limited in solution.<sup>2</sup> One of the relevant and probably the most important unresolved issue related to the HNO biological role concerns the possibility of in vivo endogenous formation of azanone. The studies of this issue are contradictory, and a definite answer is still missing.<sup>2</sup> The most accepted pathway for in vivo HNO production has been speculated to result from the enzymatic activity of heme-containing nitric oxide synthase (NOS) under particular cofactor conditions.<sup>8,9</sup> In the proposed reaction, the substrate arginine is oxidized in a heme-mediated oxygen-dependent four-electron-redox reaction to yield HNO, whose presence is argued on the basis of N<sub>2</sub>O and NH<sub>2</sub>OH detection. Additional evidence for NOS-based azanone generation includes detection of Fe(II)NO in NOS, rather than the usual ferric resting state.<sup>9,10</sup> Recently, Marletta and co-workers argued that in the last step of NO production by NOS, a

biopterin-centered radical oxidizes the Fe(II)NO to an Fe(III)NO species that allows NO to be released from the ferric iron.<sup>11,12</sup> The problem with this mechanism is that it seems unlikely that the Fe(II)–NO intermediate could actually release H<sup>•</sup>NO or <sup>3</sup>NO.<sup>11,12</sup> Another possible endogenous azanone source relies on the oxidation of hydroxylamine or other alcohol amines, such as *N*-hydroxy arginine, which are postulated to depend on the activity of several heme proteins in vivo (e.g., peroxidases or myoglobin). These are able to stabilize ferryl species (compound I and compound II), as shown by Wink and co-workers.<sup>13</sup> However, as for the NOS-based mechanism, there are several remaining unresolved questions concerning the proposed mechanism in vivo; these include understanding how the protein is driven to the formation of the key oxo ferryl species or how HNO escapes the ferric heme pocket.<sup>2</sup> Finally, there are at least two nonenzymatic proposed routes for in vivo azanone production. The first follows the decomposition of nitrosothiols by other

Received: July 4, 2013

Accepted: August 19, 2013

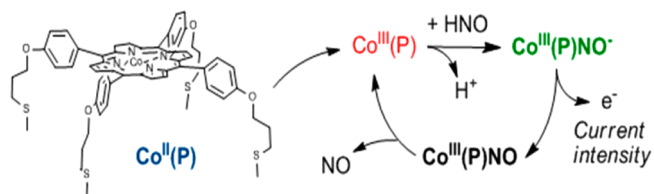
thiols (such as glutathione), as shown by several *in vitro* studies.<sup>2,14,15</sup> Second, it was recently shown that hydrogen sulfide reacts with NO (or the NO donor nitroprusside) to yield HNO.<sup>16</sup> Although the above-cited studies make a strong point for *in vivo* HNO production, it should be stressed that none of the proposed mechanisms have been undoubtedly confirmed, and that to our knowledge, there has been no report of any tissue- or cell-based azanone detection *in vivo*. This lack of certainty is primarily related to the difficulties encountered with the unequivocal and quantitative detection of HNO in real time at nanomolar or picomolar concentrations. Therefore, the development of reliable analytical methods for quantitative HNO detection is in high demand for the advancement of the biomedical and chemical research in this area.

Until recently, only indirect methods were available, the most popular being measurement of N<sub>2</sub>O concentration. However, in the past few years, several methods were developed to detect and quantify HNO.<sup>2,6,7,13,17–21</sup> Common reagents for discriminating and detecting HNO and NO rely on the use of thiols (e.g., cysteine) as blocking agents. However, chemical discrimination between species requires purification and characterization of final products.<sup>22,23</sup> In this line, Wink and co-workers developed a reliable azanone-selective assay in which the reaction products GS(O)NH<sub>2</sub> in the presence of reduced glutathione (GSH) are quantified by high-performance liquid chromatography (HPLC).<sup>13,14</sup> Another interesting approach for HNO detection relies on colorimetric or UV–vis-based methods. Very recently, King and co-workers proved that reaction of HNO with triarylphosphines produces azalides and HNO-derived amides, products which allow indirect quantification of HNO by HPLC.<sup>18</sup> Moreover, combining the phosphines with adequate carbamates, the authors were able to develop a colorimetric assay for HNO detection, up to the micromolar level, showing compatibility with physiological-like media.<sup>18</sup> Other colorimetric methods rely on the use of manganese porphyrins.<sup>6,19</sup> Schoenfisch and co-workers developed an assay based on encapsulation of a Mn porphyrin (manganese(III) *meso*-(tetrakis(4-sulfonato-phenyl)) porphyrinate, Mn<sup>III</sup>TPPS) in a xerogel film, which allows quantification of HNO in the presence of oxygen by UV–vis measurements. Time-resolved HNO concentration could be obtained at 60 s intervals and [HNO] ≈ 50 nM or more.<sup>19</sup> Manganese-reconstituted myoglobin allowed discrimination between HNO and NO in the presence of oxygen, detecting azanone at concentrations close to the nanomolar level.<sup>24</sup> The problem with the use of this type of strategy *in vivo* is that the signal to be observed (a shift in the metalloporphyrin Soret band in the UV–vis spectra) overlaps with the absorbance of any heme protein, which are the main targets under study.<sup>2</sup> Another HNO detection method has been recently developed by Lippard and co-workers, based on a fluorescent probe comprising a reporter site, which has optical properties that are well-suited for cellular imaging experiments and a tripodal coordination environment, both separated by a rigid spacer.<sup>20</sup> The complex was tested in living cells: addition of a commonly used HNO donor such as Angeli's salt (AS) to these cells increased the observed intracellular green fluorescence over the course of 10 min, which is consistent with an HNO-induced emission response. Another fluorescent probe was recently developed by Yao and co-workers, allowing the detection of HNO generated by a minimum concentration of 1 μM AS.<sup>21</sup> Toscano and co-workers have recently developed a unique method to detect HNO by membrane-inlet mass spectrometry.

The common HNO donors AS and Piloty's acid (PA) along with a newly developed donor were studied by this technique with a detection level for HNO of ≈ 50 nM.<sup>17</sup>

Finally, in a recent work from our group, we showed the first step toward the design of an azanone electrochemical sensor by covalently attaching a cobalt porphyrin to a gold electrode through Au–S bonds.<sup>25</sup> In this respect, several kinetic and structural studies have investigated the reaction of NO with both Co<sup>II</sup> and Co<sup>III</sup> porphyrins.<sup>26,27</sup> The results show that as for iron and manganese the most stable complex is the Co<sup>II</sup>NO complex, whereas the Co<sup>III</sup>NO loses the NO rapidly. Interestingly, structural characterization shows that the Co<sup>II</sup>NO species is better-represented as Co<sup>III</sup>NO<sup>−</sup>.<sup>27</sup> Thus, when azanone (<sup>1</sup>HNO/<sup>3</sup>NO<sup>−</sup>) is made to react with Co<sup>III</sup>, it directly yields the adduct, and no reductive nitrosylation occurs. The cobalt(II) 5,10,15,20-tetrakis[3-(*p*-acetylthiopropoxy) phenyl]-porphyrin (Co(P))-modified electrodes<sup>25</sup> were thoroughly characterized by XPS, STM, and electrochemical methods showing that (i) the porphyrin molecules were adsorbed in the lying-down configuration by multiple linkers binding to the gold surface, (ii) a strong gold–porphyrin interaction shifts the Co<sup>III</sup>/Co<sup>II</sup> couple ≈ 400 mV to lower potentials compared to the E<sub>1/2</sub> in solution, and (iii) as expected, while Co<sup>III</sup>(P) reacts efficiently with HNO, it does not do so with NO.<sup>25</sup> On the basis of these data, Scheme 1 was proposed in order to

**Scheme 1. Reactions Involved in the Amperometrical Detection of HNO by Co(P)**



selectively detect azanone amperometrically. According to this scheme, the resting-state electrode potential is set to 0.8 V, a value where the porphyrin is stable in the Co<sup>III</sup>(P) state and no current flow is observed. Reaction with HNO yields Co<sup>III</sup>(P)NO<sup>−</sup>, which under the described conditions is oxidized to Co<sup>III</sup>(P)NO. The resulting Co<sup>III</sup>(P)NO complex releases the NO ligand in a fast manner and yields Co<sup>III</sup>(P), which allows the catalytic cycle to start again. In the proposed mechanism, the current intensity is thus proportional to the amount of HNO that binds the Co<sup>III</sup>(P). The Co(P)-modified electrode was tested by measuring the current versus time plot at 0.8 V, showing that a few seconds after the addition of AS the current intensity increases, and it is maintained for several minutes due to the catalytic cycle, sustained by continuous HNO production from the donor.<sup>25</sup>

In the present work, we have extended the characterization of the recently developed Co(P) electrode in several key aspects related to its potential use in chemical and biological studies involving azanone. First, we performed detailed kinetic analysis of the time-resolved electrode response in the presence of well-characterized HNO sources, such as AS and TSHA, showing that it is possible by these means to obtain the corresponding reaction rate constants. Second, we analyzed the quantitative nature of the obtained signal, which shows that the Co(P) electrode can be calibrated, exhibiting a linear response in transient HNO concentration from 1 to 1000 nM. The corresponding concentrations were tested independently using

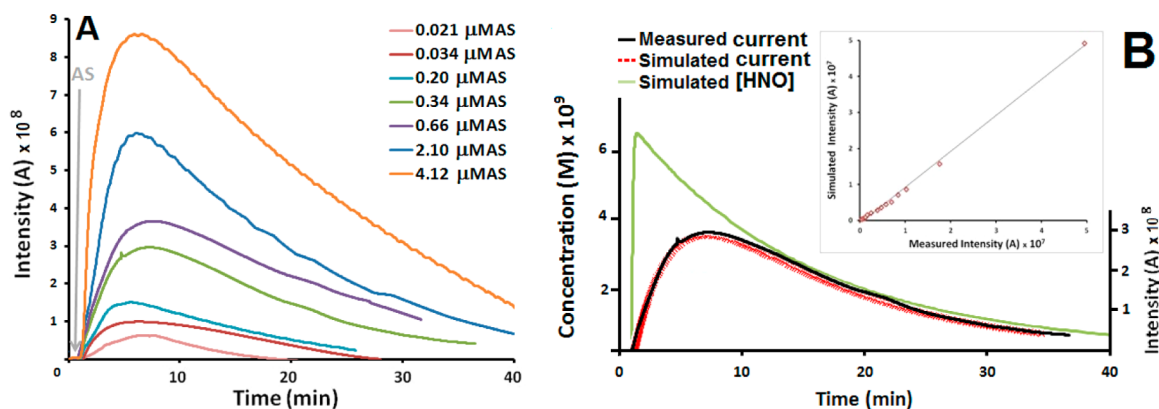


**Figure 1.** (A) Current intensity vs time plots for the Co(P)-modified electrode after the addition of increasing initial concentrations of HNO donor ( $[AS]_0$ ). Each curve corresponds to a different  $[AS]_0$ . Time of addition is indicated by the arrow. (B) Current measurement and simulated vs  $t$  (right axis; black and red, respectively) and simulated  $[HNO]$  at the same donor concentration (left axis, green,  $0.34 \mu M$ ). A slight delay is observed in the signal. Inset: measured vs simulated current at  $I_{max}$  (350 seg).

a previously developed trapping method, and the results were in excellent agreement with the results obtained amperometrically. Third, we analyzed the possible occurrence of spurious signals (or interference) due to the presence of oxygen and other reactive nitrogen and oxygen species (RNOS). The results show that several commonly expected species do not affect the electrode performance, although in the presence of  $O_2$ , the concentration of HNO decreases notably due to its known reaction with dioxygen.<sup>28</sup> Finally, in order to show its applicability to biological media, azanone was quantified using the electrode in the presence of living cells, which exhibited practically no interference. In summary, the Co(P) electrode is to our knowledge the best prospect to be used in studies looking for HNO-related chemical and biological reactions.

## MATERIALS AND METHODS

**Chemicals.** Co<sup>II</sup>(P) and cystamine were purchased from Frontier Scientific and used as received. All other reagents were purchased from Sigma-Aldrich. Angeli's salt, trioxodinitrate ( $N_2O_3^{2-}$ , AS), and *N*-hydroxy-4-methylbenzenesulfonamide (TSHA) were synthesized according to published literature procedures.<sup>28,29</sup>

**Instruments.** Cyclic voltammetry and amperometric techniques were carried out with a TEQ 03 potentiostat. A three-electrode system was used, consisting of platinum counter electrodes, Ag/AgCl as the reference electrode, and gold as the working electrode (see Figure S1). In water, the potential was measured against a Ag/AgCl reference and converted to SCE reference by using  $E(SCE) = E(Ag/AgCl) + 0.045 V$ . All procedures were similar to those previously reported by our group for working with the Co(P) electrode.<sup>25</sup>

**Kinetic Determination of AS-Derived HNO Concentrations in Solution Using Mn<sup>III</sup>TPPS Porphyrin as a Trapping Agent.** All experiments were performed at 25 °C in 0.1 M phosphate buffer (pH 7.4) containing  $10^{-4}$  M EDTA to avoid HNO catalytic decomposition by Cu<sup>II</sup> or other divalent cations. Porphyrin and donor concentrations were in the range of  $0.2$ – $2 \times 10^{-6}$  M and in a 1:1 ratio, unless otherwise stated. All reactions were unaffected by the irradiation of the sample with the light source of the spectrometer. The reaction rate was measured by following the absorbance of the metalloporphyrinates at the peak position of the Soret band (see the Supporting Information for more details).<sup>6</sup>

**HNO Electrochemical Measurements.** Current response was measured by the addition of HNO donor solutions (SA or TSHA) to the electrochemical cell. Each concentration corresponds to an independent experiment (same initial solution at the electrode cell).

**Kinetic Simulations of HNO Reactions in the Presence of the Co(P)-Modified Electrode.** Simulated reaction profiles were used to analyze the electrode response as a function of time. A set of differential equations associated with the reactions was solved with MATLAB 2009b.

**Interference Measurements.** To determine the signal obtained by the electrode in the presence of several possible interfering compounds, we measured cyclic voltammograms between 0 and 1000 mV using  $KNO_3$  as the supporting electrolyte in aerobic (i.e., air) and anaerobic media.

**Biological Media Measurements.** To determine the Co(P)-modified electrode capacity to quantitatively detect azanone in biological media, we measured the modified electrode signal obtained from AS-derived HNO in a *Xenopus* melanophore cell culture. Immortalized *Xenopus* melanophores were adherent-cultured at 27 °C in 0.7X L-15 medium, supplemented with 10% fetal bovine serum, 5  $\mu g/mL$  insulin, penicillin, streptomycin, and phenylthiourea, as described by Bruno et al.<sup>30</sup> The electrochemical measurement setup consisted of the same setup used for the in vitro studies (described in Figure S1), but the electrochemical cell consisted of the melanophore culture dish. For these measurements, the working Co(P)-modified electrode was located as close as possible to the living cells.

For more details regarding the methodology, see the Supporting Information.

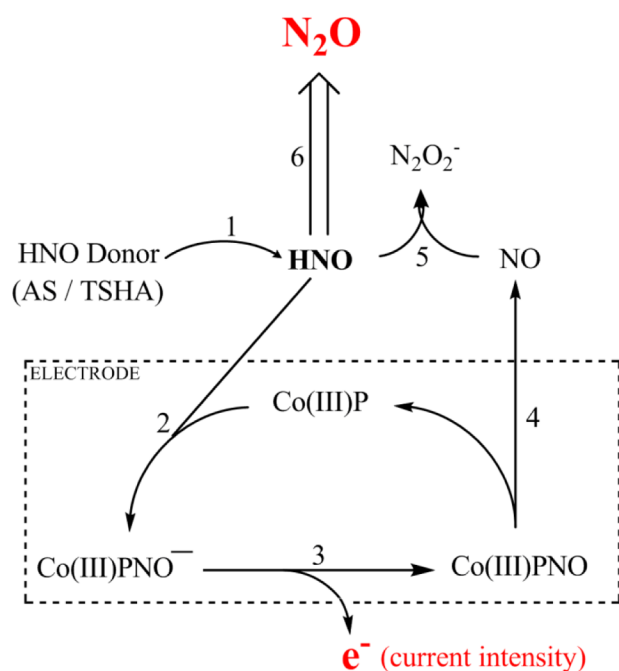
## RESULTS AND DISCUSSION

**Kinetic Analysis of the Time-Resolved Electrode Response toward HNO.** In our previous work, we showed that upon generation of azanone in solution using AS as a donor, a time-dependent electrical response can be obtained. In particular, we were able to record the change in the current intensity and to relate its value to the presence of HNO in solution (Scheme 1). The intensity current versus time plots (presented in Figure 1A) show that a few seconds after AS addition a steep rise in the signal is observed, and that the maximum rise in the amperometric signal ( $\Delta C$ ) is larger for increasing AS concentrations. In all cases, it reaches a maximum

value and subsequently decays slowly on the same time scale as the donor decomposition. The proportional increase in  $\Delta C$  for increasing donor concentrations and the signal decay shape and time scale strongly suggest that the Co(P) electrode is monitoring [HNO] in a time-resolved fashion. Therefore, we decided to analyze the shape of the plot using a kinetic model and to determine if it is possible to extract important kinetic information from the corresponding azanone-producing process.

**Kinetic Model of the Co(P) Response to AS.** We will use as the starting point in our analysis the signal produced by the HNO derived from the decomposition of Angeli's salt, as shown above. The minimal kinetic reaction model (described in Scheme 2) that can be used comprises the spontaneous

**Scheme 2. Mechanistic Reaction Scheme Considered for the Kinetic Analysis of the Electrode Response to AS-Derived Azanone (HNO)**



decomposition of the donor in order to generate HNO (reaction 1), which can dimerize to N<sub>2</sub>O (reaction 6) or react at the electrode by coordination to the Co<sup>III</sup> porphyrin (reaction 2) bound to the electrode. The resulting Co<sup>III</sup>PNO<sup>-</sup> is oxidized at the electrode, generating the measured electric current (reaction 3) and Co<sup>III</sup>PNO. In this complex, the Co–NO bond is labile, and NO is quickly released, regenerating the free porphyrin (reaction 4). Finally, NO can also react with HNO (reaction 5). For reactions 1, 2, 5, and 6, the

corresponding kinetic rate constants are known (see Table 1). HNO and NO release rates from the Co(P) (back reaction 2 and reaction 4) are not known for the present cobalt porphyrin; however, they can be reasonably approximated for the same reactions with other Co porphyrins known in the literature, adopting values of  $\approx 1 \times 10^{-3} \text{ s}^{-1}$ .

Near the electrode surface, a thin layer is established where the flow velocity is essentially zero. Mass transport takes place by diffusion alone, and thus a continuous flow is required to maintain the surface concentrations demanded by Nernst's equation. Convection maintains a constant supply of HNO at the outer edge of the diffusion layer, which is proportional to the HNO concentration in bulk solution. The observed current will thus depend on the HNO diffusion rate, the thickness of the diffusion layer, and the HNO concentrations at the electrode surface and in bulk solution. Assuming that Co(P) is wired to the electrode, that HNO binding to Co(P) is very fast ( $k_{\text{on}}$  is expected to be on the order of  $10^4 \text{ M}^{-1} \text{ s}^{-1}$ ) for a thin layer, and given that the concentration of HNO at the electrode approaches zero (since it binds and is consumed by the Co(P)), the resulting current intensity ( $i$ ) is directly proportional to azanone concentration in bulk solution [HNO], according to eq 1:

$$i_l = \frac{nFAD_{\text{HNO}}}{\delta} C_{\text{HNO}} = k_{e\text{HNO}} C_{\text{HNO}} \quad (1)$$

where  $n$  is the number of electrons per mole of HNO,  $F$  is Faraday's constant,  $A$  is the electrode surface area ( $\text{cm}^2$ ),  $D_{\text{HNO}}$  is the diffusion coefficient for azanone, and  $\delta$  is the thickness of the diffusion layer. Since  $nFAD_{\text{HNO}}$  and  $\delta$  are constants for a given system, we will group them in the above-mentioned system-dependent effective rate  $k_{e\text{HNO}}$ . It is important to note that although this model is based on an oversimplified picture of the diffusion layer, it nevertheless provides a reasonable approximation of the relationship between current and the variables that affect it and, in this case, the bulk concentration of HNO (see below).

Numerically solving the set of differential equations that describes the reaction in Scheme 2 using the values from Table S2, a very good fit of the simulated intensity to the measured current versus time plot is obtained (Figure 1B). To have a more stringent test of our model, we performed the same analysis for all measured donor concentrations. In all cases, there is an excellent fit between observed and computed  $I$  versus time plots. The resulting plot of the measured  $\Delta C$  versus the computed  $\Delta C$  (inset of Figure 1B) shows the expected linear relationship with a slope of 0.9977 in the entire tested range ( $R^2 = 0.9973$ ). Finally, solving the set of equations, allows us to understand the resulting plot shape. As shown in Figure 1B (and Figure S4), the fast signal rise reflects the initial maximum HNO concentration produced by AS decomposition

**Table 1. Kinetic Reactions Used To Model the Electrochemical Response to AS**

reaction no.	reaction	constant value		refs
1	Angeli's salt $\rightarrow$ HNO	$0.0023 \text{ s}^{-1}$	$k_{\text{dec}}$	6,7,24,31,32
2	$\text{Co}^{\text{III}}\text{P} + \text{HNO} \leftrightarrow \text{Co}^{\text{III}}\text{PNO}^- + \text{H}^+$	$3 \times 10^4 \text{ M}^{-1} \text{ s}^{-1}$	$k_{\text{on}}$	6
-2		$3.5 \times 10^{-3} \text{ s}^{-1}$	$k_{\text{off}}$	this paper
3	$\text{Co}^{\text{III}}\text{PNO}^- \rightarrow \text{Co}^{\text{III}}\text{PNO} + \text{e}^-$	$5.4 \times 10^{-4} \text{ s}^{-1}$	$k_{\text{ox}}$	this paper
4	$\text{Co}^{\text{III}}\text{PNO} \rightarrow \text{Co}^{\text{III}}\text{P} + \text{NO}$	$5.2 \times 10^{-3} \text{ s}^{-1}$	$k_{\text{off}}$	27
5	$\text{HNO} + \text{NO} \rightarrow \text{N}_2\text{O}_2^- + \text{H}^+$	$5.8 \times 10^6 \text{ M}^{-1} \text{ s}^{-1}$	$k_{\text{NO}_-\text{HNO}}$	36
6	$2\text{HNO} \rightarrow \text{N}_2\text{O} + \text{H}_2\text{O}$	$8 \times 10^6 \text{ M}^{-1} \text{ s}^{-1}$	$k_{\text{dim}}$	33–35

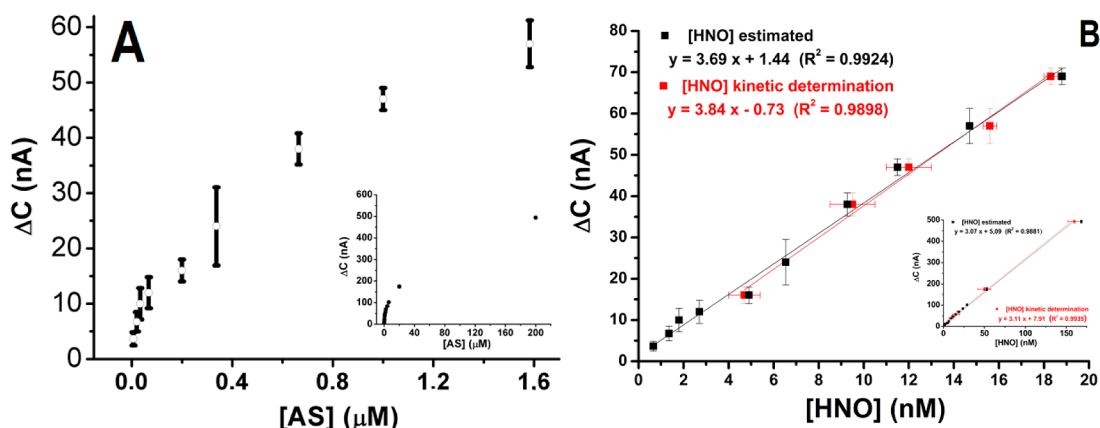


**Figure 2.** (A)  $\Delta C$  intensity signal (nA) detected by Co(P)-modified gold electrodes as a function of AS concentration (range: 0–1.6  $\mu\text{M}$ ). Inset: 0–200  $\mu\text{M}$  range. (B) The red plot shows the calibration of the current intensity using the method of Schoenfisch et al. through eq S4. Note that due to instrumental limitations (Soret band intensity), [HNO] cannot be measured by this method below 4 nM. The black plot shows the calibration of the current intensity by calculating [HNO] through the simulation described above. The [HNO] range is  $\approx 1$ –20 nM. Inset: same as above for the [HNO] range of  $\approx 1$ –150 nM. Note that the plot is practically linear even for the highest [HNO].

at the working pH and its time delay is related to its diffusion to the electrode surface through the Nernst diffusion layer plus the time involved in the formation of the  $[\text{Co}^{\text{III}}\text{HNO}]^-$  complex. The exponential-like decay simply reflects the decay in bulk [HNO] as a consequence of the exponential decay in AS concentration (its half-life under the same conditions is  $\approx 15$  min and follows first-order kinetics similar to the observed signal). In summary, the electrode signal reflects the actual azanone concentration in a time-resolved fashion, thus allowing the performance of kinetic measurements of HNO production/consumption.

*Using the Co(P) Electrode Time-Resolved Signal To Determine Kinetic Rates Associated with HNO-Related Reactions.* To analyze the performance of the present electrode (the associated differential set of equations and obtained rate constants) as a method to determine unknown rate constants associated with HNO reactions, we measured the electrode response to a solution of known TSHA concentration. The resulting plot (shown in Figure S5) was analyzed using the previously described set of equations, leaving the model free-to-fit and allowing the determination of the TSHA decomposition rate. The obtained value of  $5.5 \times 10^{-4} \text{ s}^{-1}$  at 25  $^{\circ}\text{C}$  is in excellent agreement with the reported value of  $4.4 \times 10^{-4} \text{ s}^{-1}$ , showing that the Co(P) electrode and the associated kinetic model are appropriate to analyze kinetically reactions involving HNO.

**Determination of the Dynamic Range for Quantitative Amperometric Azanone (HNO) Detection Using the Co(P) Electrode.** We now turn our attention to the determination of the dynamic range (i.e., the range of bulk HNO concentrations) that our electrode is able to detect quantitatively. The aim of this analysis is not to determine kinetic rates (as shown above) but to detect and quantify the maximum amount of azanone present in a given system at any time. To this end, we first calibrated the peak response ( $\Delta C$ ) with known [HNO] in solution. It is important to note that due to its intrinsic reactive property, precise determination of azanone concentrations is not easy, and we used three different approaches to determine it. First, as previously shown by several studies from our group and others,<sup>2,6,7,23,28</sup> as a result of the fast equilibrium established between the continuous azanone production by the spontaneous donor decomposition

and its dimerization, when the donor starts to decompose, a peak steady-state instantaneous azanone concentration is achieved that subsequently slowly decays as the donor is consumed. Moreover, since dimerization is second-order in [HNO], the higher the HNO concentration the faster it dimerizes, resulting in an inverse-square relation between initial donor and peak azanone concentration, which can be approximated by eq 2:

$$[\text{HNO}] = \sqrt{\frac{k_d[\text{donor}]}{2k_h}} \quad (2)$$

where  $k_d$  is the first-order rate constant of the donor decomposition and  $k_h$  is the bimolecular rate constant of HNO dimerization. A direct consequence of this relation is that high concentrations of azanone cannot be achieved with relative slow donors such as AS. The above-described inverse-square relation between donor and peak [HNO] and the apparent upper limit to azanone concentration are clearly evidenced in Figure 2A, where the measured  $\Delta C$  is plotted against initial AS concentration. On the basis of the obtained peak signal and eq 2, a first calibration of the electrode response as a quantitative HNO sensor can be performed by plotting measured  $\Delta C$  from different initial donor concentrations against peak [HNO] as determined by eq 2, showing that the electrode has a linear response in the 1–150 nM range (Figure 2B). In order to have a second, more accurate estimation of peak [HNO], we also computed it using the kinetic scheme described previously. The resulting  $\Delta C$  versus estimated [HNO] calibration curve, shown by the black dots in Figure 2B, shows an excellent linear response ( $R^2 = 0.98998$ ) in the 1–150 nM range that is able to detect peak HNO concentrations as small as 0.7 nM. The difference between the estimations of azanone concentration using eq 2 and the kinetic scheme is that in using eq 2 slightly higher [HNO] values are obtained for a given donor concentration, and the difference with the kinetic model estimation increases with increasing donor concentrations.

A third way to determine the peak concentration of HNO can be performed experimentally by monitoring the reaction of azanone with the trapping agent  $\text{Mn}^{\text{III}}\text{TTPS}$  and HNO in anaerobic media, as previously reported by Schoenfisch et al.<sup>19</sup> In this method, peak [HNO] is determined from the relation

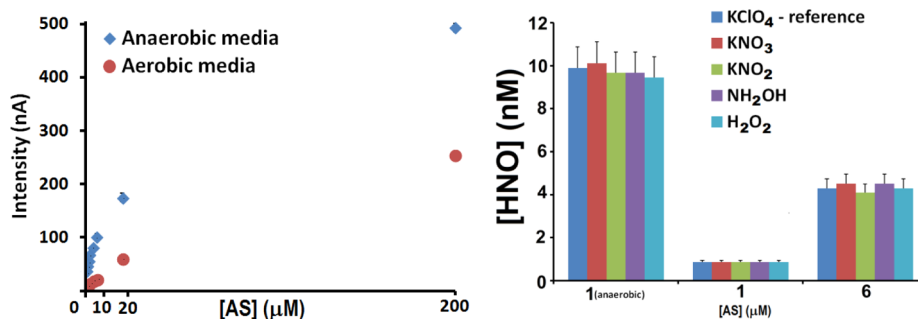


**Figure 3.** (Left panel)  $\Delta C$  values obtained for different initial AS concentrations in anaerobic (blue) and aerobic (red) media. (Right panel) [HNO] detected by AS decomposition in the presence of any of the tested RNOS ( $\text{KNO}_3$ ,  $\text{KNO}_2$ ,  $\text{NH}_2\text{OH}$ , or  $\text{H}_2\text{O}_2$ ) in both anaerobic (left) and aerobic (middle and right) media.

between the observed nitrosyl porphyrin production rate ( $\text{dMn}^{\text{II}}(\text{NO})\text{TPPS}/\text{dt}$ ) and the corresponding bimolecular rate constant ( $k_{\text{on}}$ ) for the association reaction, according to eq S4. Therefore, in order to determine peak [HNO] for each AS concentration used to obtain the  $\Delta C$  value reported in Figure 2B, we measured the corresponding nitrosyl manganese porphyrin production rate for each donor concentration using UV–vis spectroscopy (see Materials and Methods and SI for details), and all peak azanone concentrations were determined from the measured rate. The resulting experimental azanone concentration determinations were used to plot the obtained  $\Delta C$  values versus [HNO] with red dots in Figure 2B. The plot nicely shows that the [HNO] values obtained by using the kinetic simulation are very similar to those experimentally determined following the described procedure and yield a similar calibration curve. It is also important to note that due to limitations in the UV–vis signal used to measure the nitrosyl porphyrin formation rate, the chemical method cannot be used for AS values below  $0.2 \mu\text{M}$  (corresponding to an HNO concentration of  $\approx 5 \text{ nM}$ ). In summary, independent of the method used to determine or estimate the azanone concentration in the reaction systems, the results from Figure 2B clearly show that using the Co(P) electrode, HNO can be reliably and quantitatively determined in the low nanomolar range (as low as  $1 \text{ nM}$ ) and demonstrates a linear response to peak [HNO] in the  $1\text{--}1000 \text{ nM}$  range (complete data in SI).

Finally, having performed an analysis of the signal shape and a calibration curve that relates the electrochemical signal with the HNO concentration, we can actually determine how much of the azanone in solution is reacting with the electrode (and thus also determine how much NO is released as a side product by Co(P) in the electrode). The area under the curve of the current versus time plot for a given time interval allows determination of the actual number of HNO molecules that are reduced to NO by Co(P). The kinetic simulations show that the Co(P) turnover rate is  $\approx 10 \text{ ms}$ . Considering this time interval, for an initial AS concentration of  $340 \text{ nM}$ , the peak intensity would correspond to  $2.49 \times 10^{-13} \text{ mol}$  of Co(P) electrode bound and oxidized HNO. In this system (total volume =  $5 \text{ mL}$ ), peak bulk [HNO] corresponds to a maximum amount of  $3.27 \times 10^{-11} \text{ mol}$  of free HNO in solution. Thus, the Co(P) electrode is reacting with  $<1\%$  of the available HNO molecules. The same type of analysis allows us to determine for the Co(P) electrode how far it is from saturation (when all porphyrin molecules are bound to HNO). Previously, we determined that each electrode is covered with a surface concentration of  $4.3 \times 10^{-12} \text{ mol}/\text{cm}^2$ .<sup>25</sup> Therefore, an electrode having a total surface of  $1.4 \text{ cm}^2$  could react with

an azanone bulk concentration up to  $5 \mu\text{M}$ , which is far above the measured calibration curve.

### Analysis of Possible Spurious Signals Due to Other Small Molecule Interactions with the Co(P) Electrode.

**Electrode Response in the Presence of Oxygen.** Oxygen is a ubiquitous player in any physiological media, and although tissue- and cell-based studies can be performed under anaerobic conditions, we decided to test the electrode response under air atmosphere and compare it with the above-shown results. Oxygen reacts slowly with HNO. The corresponding bimolecular reaction has a rather small rate constant of  $k \approx 10^3 \text{ M}^{-1} \text{ s}^{-1}$ <sup>36</sup> because the reaction involves spin-crossing. Strikingly, the reaction product is still unknown.<sup>33</sup> Figure 3A (Table S1) presents the obtained  $\Delta C$  values for different initial AS concentrations in anaerobic and aerobic media. At first sight, the resulting plot clearly shows that the electrode response is notably lower in the presence of oxygen. In the case of an initial AS concentration of  $1 \mu\text{M}$ , which corresponds to peak [HNO] of  $\approx 10 \text{ nM}$  in anaerobic media, oxygen scavenges 90% of the azanone, resulting in a measured peak [HNO] of only  $\approx 1 \text{ nM}$ , as determined by the Co(P) electrode signal (see Table S1 for more details). Thus, although as expected oxygen scavenges bulk HNO, the experiment demonstrates that azanone can still be detected and quantified in the presence of high concentrations of oxygen, such as those found in ambient air.

### Electrode Response in the Presence of Other Biologically Relevant Reactive Nitrogen and Oxygen Species (RNOS).

Besides oxygen, other biologically relevant RNOS could interfere or react with the Co(P) electrode, giving rise to a spurious signal that could mask or deplete the HNO signal, or, even worse, yield a false positive (i.e., a significant  $\Delta C$  in the absence of HNO). In order to analyze possible effects on the signal of RNOS found in common physiological media, we measured the bare and Co(P)-modified electrode response under several conditions. First, we performed cyclic voltammograms of a bare gold electrode in the presence of  $\text{KNO}_3$  (as electrolyte) in anaerobic and aerobic media in the presence of the following molecules:  $\text{NaNO}_2$  ( $0.1 \text{ M}$ ),  $\text{H}_2\text{O}_2$  ( $0.1 \text{ M}$ ), and  $\text{NH}_2\text{OH}$  ( $0.1 \text{ M}$ ), obtaining the same voltammogram in all cases. Moreover, we also performed the measurements with  $\text{KClO}_4$  instead of  $\text{KNO}_3$ , obtaining the same results (data not shown). These results show that none of the tested molecules yields an appreciable electrochemical signal in the Co(P) working range using a bare gold electrode in the electrode working conditions. Second, we measured the Co(P) electrode response ( $\Delta C$ ) to the addition of AS in both aerobic and anaerobic media in the presence of each mentioned RNOS at

0.1 M. It is important to perform the reactions in aerobic media because the tested RNOS may react with free oxygen yielding other RNOS that could either scavenge azanone or give rise to spurious signal (false positive). The corresponding results, presented in Figure 3B (Table S2), show that measured  $\Delta C$  is completely independent of the presence of any of the tested RNOS ( $\text{KNO}_3$ ,  $\text{KNO}_2$ ,  $\text{NH}_2\text{OH}$ , and  $\text{H}_2\text{O}_2$ ), in both anaerobic (left) and aerobic (middle and right) media. Furthermore, the Co(P) electrode also retains the azanone concentration-dependent response. Concerning  $\text{NH}_2\text{OH}$ , it is important to note that in our experimental conditions we were working at pH 7, where the predominant species is by far  $^1\text{HNO}$ . Cooper et al.<sup>37</sup> showed that hydroxylamine reacts with azanone to yield equimolar quantities of  $\text{N}_2$  and  $\text{H}_2\text{O}$ , but this occurs at a basic pH, where the reacting species is most probably  $^3\text{NO}^-$ . Thus, under the present conditions, hydroxylamine is not expected to act as an azanone consuming agent.

In summary, the Co(P) electrode is selective for HNO, while other nitrogen oxoanions such as NO (as shown in our previous work),<sup>25</sup> oxygen, hydrogen peroxide, and their possible reaction products do not seem to interfere with the electrode signal, showing that the detection method is robust and reliable.

**Testing the Co(P) Electrode Response in Biological Media.** We next assessed the ability of the Co(P)-modified electrode to operate in real biological media, under conditions similar to those used by Lippard and Yao.<sup>20,21</sup> In this regard, we used *Xenopus melanophores* (see Materials and Methods) in a dish. We then built a working/reference/counter electrode setup, as shown in Figure S1. In the corresponding conditions, the working electrode is in direct and close contact with the cells embedded in physiological media. Under these conditions, no significant current is measured when the electrode is set to the working potential of 0.8 V, showing that biological media do not give rise to any spurious signal. We then analyzed the electrode response in contact with the living cells upon addition of varying amounts of AS. We also measured the same response using the cell culture media alone (i.e., without cells) after performing a cell lysate. As in previous cases, the experiments were performed in anaerobic (except for intact cells) and aerobic media. The results are shown in Figure 4 (Table S3).

The results from Figure 4 show that the Co(P) electrode is biocompatible and able to detect and quantify HNO in

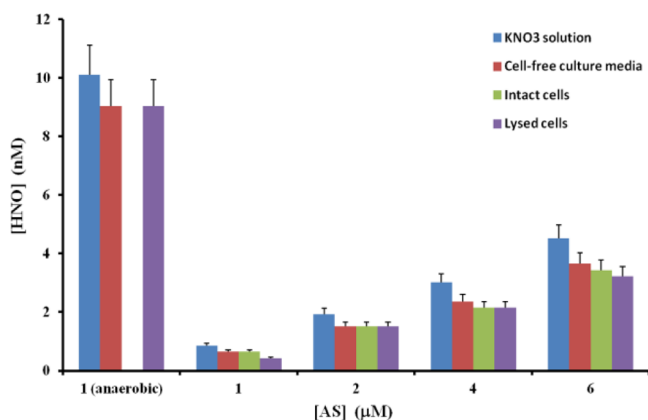


**Figure 4.** [HNO] produced by AS decomposition in the presence of *Xenopus melanophore* cell culture. Experiments were performed under air atmosphere unless otherwise noted. Only the lysed cells were measured anaerobically (left).

biological media, including intact or lysed cells, and in the presence of oxygen. It is interesting to note that the signal is slightly reduced in the following order:  $\text{KNO}_3$  solution > cell-free culture media > intact cells > lysed cells. The small signal decrement is more evident for higher concentrations of HNO. This result is completely reasonable and expected because HNO is a highly reactive molecule, and the higher the level of other HNO-reacting molecules, the less HNO is able to react with the electrode. The presence of cells (and lysed contents) results in an increase (a larger increase with lysed contents) of molecules reactive to HNO (heme proteins, thiols, and others). These experiments show that the modified electrode still works in the presence of cells and cell contents, although it remains to be shown that it can detect HNO inside the cells. In the near future, we plan to perform further studies concerning possible interference or HNO-consuming reactions by biological thiols like GSH. Finally, our results show that in a cell lysate under air atmosphere, HNO can be detected at the level of up to 10 nM.

## CONCLUSIONS

Azanone can be trapped in a fast manner by a  $\text{Co}^{\text{III}}$  porphyrin covalently attached to a gold surface. Due to this unique property, an electrode based on these materials can be constructed that allows selective detection and quantification of HNO in a time-resolved fashion (with 1 s resolution). It is possible to obtain kinetic information about the reactions involving azanone at low nanomolar concentrations and up to 1000 nM in the presence of putative interferences (including NO and other RNOS) in both anaerobic and aerobic media. The electrode can also be used in living tissue such as cultured cells with the advantage that it can be introduced in the culture dish and removed after the measurements without disrupting or contaminating the tissue. In summary, the Co(P) electrode is to our knowledge the best choice to be used in studies investigating HNO-related chemical and biological reactions. Considering the biological, pharmacological, and chemical relevance of azanone and its elusive nature, the development of this sensor will be crucial for the long-awaited assessment of HNO as an endogenous molecule. Next steps toward this aim would be to miniaturize the electrode and to lower the detection limit to the picomolar scale. This would allow application of this technology to studies of living tissue (e.g., aortic rings) or cells that could produce HNO in culture (e.g., vascular smooth muscle cells, macrophages, etc.) in an effort to reveal the endogenous production of HNO.

## ASSOCIATED CONTENT

### Supporting Information

Kinetic determination of AS-derived HNO concentrations in solution using the Mn porphyrin, TSHA decomposition rate, Co(P) electrode response ( $\Delta C$ ) to the addition of the azanone donor, AS, in anaerobic and aerobic media, electrode response in the presence of other biological molecules, test of the Co(P) electrode response in biological media, and four supplementary figures. This material is available free of charge via the Internet at <http://pubs.acs.org>.

## AUTHOR INFORMATION

### Corresponding Authors

\*E-mail: [doctorovich@qi.fcen.uba.ar](mailto:doctorovich@qi.fcen.uba.ar). Fax: (5411)-4576-3341.

Tel.: (5411)-4576-3378 (ext. 116).

\*E-mail: [marcelo@qi.fcen.uba.ar](mailto:marcelo@qi.fcen.uba.ar).

## Notes

The authors declare no competing financial interest.

## ACKNOWLEDGMENTS

This work was financially supported by the Universidad de Buenos Aires (UBA) (UBACYT W583 and 2010-12), ANPCyT (PICT 2010-2649 and 2010-416), CONICET (PIP1207 and 112-201001-00125), and the Bunge y Born Foundation. D.E.B., D.E.W., M.A.M., and F.D. are members of CONICET.

## REFERENCES

- (1) Miranda, K. M. *Coord. Chem. Rev.* **2005**, *249*, 433–455.
- (2) Doctorovich, F.; Bikiel, D.; Pellegrino, J.; Suárez, S. A.; Larsen, A.; Martí, M. A. *Coord. Chem. Rev.* **2011**, *255*, 2764–2784.
- (3) Bartberger, M. D.; Fukuto, J. M.; Houk, K. N. *Proc. Natl. Acad. Sci. U.S.A.* **2001**, *98*, 2194–2198.
- (4) Ford, P. C. *Inorg. Chem.* **2010**, *49*, 6226–6239.
- (5) Hoshino, M.; Laverman, L.; Ford, P. C. *Coord. Chem. Rev.* **1999**, *187*, 75–102.
- (6) Martí, M. A.; Bari, S. E.; Estrin, D. A.; Doctorovich, F. *J. Am. Chem. Soc.* **2005**, *127*, 4680–4684.
- (7) Suárez, S. A.; Martí, M. A.; De Biase, P. M.; Estrin, D. A.; Bari, S. E.; Doctorovich, F. *Polyhedron* **2007**, *26*, 4673–4679.
- (8) Adak, S.; Wang, Q.; Stuehr, D. J. *J. Biol. Chem.* **2000**, *275*, 33554–33561.
- (9) Schmidt, H. H. W.; Hofmann, H.; Schindler, U.; Shutenko, Z. S.; Cunningham, D. D.; Feelisch, M. *Proc. Natl. Acad. Sci. U.S.A.* **1996**, *93*, 14492–14497.
- (10) Hobbs, A. J.; Fukuto, J. M.; Ignarro, L. J. *Proc. Natl. Acad. Sci. U.S.A.* **1994**, *91*, 10992–10996.
- (11) Stoll, S.; NejatyJahromy, Y.; Woodward, J. J.; Ozarowski, A.; Marletta, M. A.; Britt, R. D. *J. Am. Chem. Soc.* **2010**, *132*, 11812–11823.
- (12) Woodward, J. J.; Nejatyjahromy, Y.; Britt, R. D.; Marletta, M. A. *J. Am. Chem. Soc.* **2010**, *132*, 5105–5113.
- (13) Donzelli, S.; Espey, M. G.; Flores-Santana, W.; Switzer, C. H.; Yeh, G. C.; Huang, J.; Stuehr, D. J.; King, S. B.; Miranda, K. M.; Wink, D. A. *Free Radical Biol. Med.* **2008**, *45*, 578–584.
- (14) Donzelli, S.; Espey, M. G.; Thomas, D. D.; Mancardi, D.; Tocchetti, C. G.; Ridnour, L. A.; Paolucci, N.; King, S. B.; Miranda, K. M.; Lazzarino, G.; Fukuto, J. M.; Wink, D. A. *Free Radical Biol. Med.* **2006**, *40*, 1056–1066.
- (15) Stoyanovsky, D. A.; Tyurina, Y. Y.; Tyurin, V. A.; Anand, D.; Mandavia, D. N.; Gius, D.; Ivanova, J.; Pitt, B.; Billiar, T. R.; Kagan, V. E. *J. Am. Chem. Soc.* **2005**, *127*, 15815–15823.
- (16) (a) Filipovic, M. R.; Eberhardt, M.; Prokopovic, V.; Mijuskovic, A.; Orescanin-Dusic, Z.; Reeh, P.; Ivanovic-Burmazovic, I. *J. Med. Chem.* **2013**, *56* (4), 1499–1508. (b) Filipovic, M. R.; Miljkovic, J. L.; Nauser, T.; Royzen, M.; Klos, K.; Shubina, T.; Koppenol, W. H.; Lippard, S. J.; Ivanović-Burmazović, I. *J. Am. Chem. Soc.* **2012**, *134*, 12016–12027.
- (17) Cline, M. R.; Tu, C.; Silverman, D. N.; Toscano, J. P. *Free Radical Biol. Med.* **2011**, *50*, 1274–1279.
- (18) Reisz, J. A.; Zink, C. N.; King, S. B. *J. Am. Chem. Soc.* **2011**, *133*, 11675–11685.
- (19) Dobmeier, K. P.; Riccio, D.; Schoenfish, M. H. *Anal. Chem.* **2008**, *80*, 1247–1254.
- (20) Rosenthal, J.; Lippard, S. J. *J. Am. Chem. Soc.* **2010**, *132*, 5536–5537.
- (21) Zhou, Y.; Liu, K.; Li, J.-Y.; Fang, Y.; Zhao, T.-C.; Yao, C. *Org. Lett.* **2011**, *13*, 2357–2360.
- (22) Shoeman, D. W.; Shirota, F. N.; DeMaster, E. G.; Nagasawa, H. *T. Alcohol* **2000**, *20*, 55–59.
- (23) Pino, R. Z.; Feelisch, M. *Biochem. Biophys. Res. Commun.* **1994**, *201*, 54–62.
- (24) Boron, I.; Suárez, S. A.; Doctorovich, F.; Martí, M. A.; Bari, S. E. *J. Inorg. Biochem.* **2011**, *105*, 1044–1049.
- (25) Suárez, S. A.; Fonticelli, M. H.; Rubert, A. A.; de La Llave, E.; Scherlis, D.; Salvarezza, R. C.; Martí, M. A.; Doctorovich, F. *Inorg. Chem.* **2010**, *49*, 6955–6966.
- (26) Farmer, P. J.; Sulc, F. *J. Inorg. Biochem.* **2005**, *99*, 166–184.
- (27) Roncaroli, F.; van Eldik, R. *J. Am. Chem. Soc.* **2006**, *128*, 8042–8053.
- (28) Miranda, K. M.; Paolucci, N.; Katori, T.; Thomas, D. D.; Ford, E.; Bartberger, M. D.; Espey, M. G.; Kass, D. A.; Feelisch, M.; Fukuto, J. M.; Wink, D. A. *Proc. Natl. Acad. Sci. U.S.A.* **2003**, *100*, 9196–9201.
- (29) Bonner, F. T.; Degani, H.; Akhtar, M. J. *J. Am. Chem. Soc.* **1981**, *103*, 3739–3742.
- (30) Bruno, L.; Salierno, M.; Wetzler, D. E.; Despósito, M. A.; Levi, V. *PLoS One* **2011**, *6*, e18332-1–e18332-8.
- (31) Bari, S. E.; Martí, M. A.; Amorebieta, V. T.; Estrin, D. A.; Doctorovich, F. *J. Am. Chem. Soc.* **2003**, *125*, 15272–15273.
- (32) Miranda, K. M.; Dutton, A. S.; Ridnour, L. A.; Foreman, C. A.; Ford, E.; Paolucci, N.; Katori, T.; Tocchetti, C. G.; Mancardi, D.; Thomas, D. D.; Espey, M. G.; Houk, K. N.; Fukuto, J. M.; Wink, D. A. *J. Am. Chem. Soc.* **2005**, *127*, 722–731.
- (33) Shafirovich, V.; Lymar, S. V. *Proc. Natl. Acad. Sci. U.S.A.* **2002**, *99*, 7340–7345.
- (34) Bonner, F. T.; Hughes, M. N.; Poole, R. K.; Scott, R. I. *Biochim. Biophys. Acta* **1991**, *1056*, 133–138.
- (35) Akhtar, M. J.; Lutz, C. A.; Bonner, F. T. *Inorg. Chem.* **1979**, *18*, 2369–2375.
- (36) Lymar, S. V.; Shafirovich, V.; Poskrebyshev, G. A. *Inorg. Chem.* **2005**, *44*, 5212–5221.
- (37) Cooper, J. N.; Chilton, J. E.; Powell, R. E. *Inorg. Chem.* **1970**, *9*, 2303–2304.